

First Principles Investigations in the Carbon-silicon System of Novel Tetragonal C_8 and Si_8 Allotropes, and Binary Si_2C_6 and Si_4C_4 Phases

Samir F Matar*

Lebanese German University (LGU), Sahel-Alma, Jounieh, Lebanon

***Corresponding Author:** Samir F Matar, Lebanese German University (LGU), Sahel-Alma, Jounieh, Lebanon.

Received: July 21, 2022

Published: July 28, 2022

© All rights are reserved by **Samir F Matar**.

Abstract

Within the carbon-silicon system, novel tetragonal C_8 and Si_8 allotropes and two silicon carbides Si_2C_6 and Si_4C_4 are devised. The propositions are based on density functional theory (DFT) calculations of template structures, optimized to ground state energies and subsequently derived physical properties. All four phases belong to primitive tetragonal space group $P-4m2$ N°115 characterized by large c/a tetragonality ratio. The structures consist of corner sharing C_4 and Si_4 tetrahedra highlighting covalent (in C_8) and polar covalent (in silicon carbides) chemical systems illustrated with charge density projections. C_8 is identified as ultra-hard with a Vickers hardness (H_v) amounting to 113 GPa, a result assigned to the large tetragonality ratio. Oppositely, Si_8 allotrope is found soft with $H_v = 13$ GPa alike cubic Si, and Si_4C_4 is identified with $H_v = 33$ GPa alike experimental SiC. Larger C-content Si_2C_6 is identified as super-hard with $H_v = 51$ GPa. All new phases are mechanically (elastic constants with bulk and shear moduli) and dynamically (phonon band structures) stable. The electronic band structures are characteristic of insulating C_8 with a large band gap of about 5 eV like diamond, and semi-conducting Si_2C_6 , Si_4C_4 , and Si_8 with band gaps of ~ 1 eV. The results are claimed as enriching further the Si-C system with novel materials aimed at diverse electronic and mechanic applications.

Keywords: DFT; Carbon; Silicon; Silicon Carbide; Super-hard; Elastic Constants; Phonons

Introduction and Context

The chemistry of carbon and silicon, major elements in nature, is ruled by three main factors involving:

- The difference of -Pauling- electronegativities with $\chi(C) = 2.55 > \chi(Si) = 1.80$ leading to polar Si-C bonds, i.e., with the trend of charge transfer $Si \rightarrow C$;
- The covalent radius, larger for Si with respect to C: $r(Si) = 1.14 \text{ \AA}$ versus $r(C) = 0.76 \text{ \AA}$ resulting from one extra shell for Si, i.e., with Si ($1s^2, 2s^2, 2p^6, 3s^2, 3p^2$) versus C ($1s^2, 2s^2, 2p^2$), resulting into more compressible Si as such as well as Si-based compounds as silicon carbide examined herein; and
- The tetrahedral coordination (sp^3 -like), common to Si and C.

In this context, diamond is the hardest material while isostructural silicon is soft and the equiatomic SiC shows intermediate hardness; it is considered as abrasive [1]. Regarding the valence electron count (external shell) C, Si and SiC as well as newly devised Si_2C_6 herein (vide infra) are isoelectronic with integer multiples of 4 (i.e., 32). In fact, 8 electrons are needed to form the relevant stable chemical system, i.e., diamond (C_2), intrinsic semiconductor silicon (Si_2), and silicon carbide (SiC). All systems are expected to have similar structural and electronic structures, i.e., insulating-like diamond, intrinsic semi-conductor Si and semi-conducting silicon carbide, the gap opening being due to the saturation of the valence band VB with pair integer multiple of 8.

Structurally, the extended three-dimensional 3D structures are characterized by the arrangement of corner sharing C₄/Si₄ tetrahedra where the angle ∠C-C-C = ∠Si-Si-Si = ∠C-Si-C = 109.47° highlighting sp³-like hybridization.

Recent research efforts endeavored to identify novel allotropes of carbon close to diamond thanks to modern materials research software as CALYPSO [2] and USPEX [3]. However, accurate investigations based on energy can be better achieved within a quantum mechanical framework. The most successful one is the Density Functional Theory (DFT) devised in two papers: in 1964 for the theoretical framework by Hohenberg and Kohn [4] and followed in 1965 by Kohn and Sham [5] where the so-called KS equations started the efficient solutions of the system wave equation thanks to calculation codes built around the DFT (cf. next section).

Based on DFT and crystal chemistry rationale, we recently proposed a novel ultra-hard carbon allotrope: tetragonal C₄ close to diamond (space group *I-4m2* ; N°119) and defined it as the simplest ‘seed’ of corner sharing carbon tetrahedra, leading to propose large cells for doping through substitutions and insertions [6]. In this context, the purpose of this work is to present the crystal structure and the physical properties of a novel extended carbon network of corner sharing tetrahedra derived from C₄, specifically tetragonal C₈ depicted in figure 1a and identified in a different space group: *P-4m2* N°115 (cf. Table 1). In a second step the C₈ structural setup was used to devise new Si₂C₆ (Figure 1b), Si₄C₄ (Figure 1c), and Si₈ (Figure 1d). In fact, in the C-Si system only the equiatomic SiC is known, however recent works reported on SiC₃ stoichiometry in a molecule [7] and we propose herein a stable cohesive crystal structure for Si₂C₆ based on C₈ template. Such exercise was successfully undertaken to model rarely occurring tricarbon molecule C₃ in the solid state, leading to identify a novel ultrahard carbon allotrope [8].

All four novel phases were characterized as cohesive and stable mechanically (elastic constants) and dynamically (phonon band structure). Particularly, C₈ is shown to be ultra-hard alike diamond, followed by the carbon rich Si₂C₆, identified with large hardness, and then Si₄C₄. On the contrary, Si₈ is found soft with properties close to experiment. Their isoelectronic characteristics are illustrated with insulating (C₈) to semi-conducting (Si₂C₆, Si₄C₄, and Si₈).



Figure 1: Crystal structures of the tetragonal phases. a) C₈, b) Si₂C₆, c) Si₄C₄, and d) Si₈ highlighting the corner-sharing tetrahedral 3D arrangement. Blue and brown spheres represent silicon and carbon, respectively.

a) C₈ and Si₈ (Figure 1a and 1d).
 C₈ : a = b = 2.519; c = 7.126
 Si₈ : a = b = 3.864; c = 10.933

| Atomic site | Wyckoff | x | y | z |
|-------------|---------|---|---|-------|
| C1 or Si1 | 1a | 0 | 0 | 0 |
| C2 or Si2 | 1d | 0 | 0 | ½ |
| C3 or Si3 | 2f | ½ | ½ | ¼ |
| C4 or Si4 | 2g | ½ | 0 | 0.125 |
| C5 or Si5 | 2g | ½ | 0 | 0.625 |

d(C-C) = 1.54 ; d(Si-Si) = 2.37

b) Si₂C₆ (Figure 1b).
 a = b = 2.794; c = 8.207

| Atomic site | Wyckoff | x | y | z |
|-------------|---------|---------------|---------------|---------------|
| Si1 | 1a | 0 | 0 | 0 |
| Si2 | 1d | 0 | 0 | $\frac{1}{2}$ |
| C1 | 2f | $\frac{1}{2}$ | $\frac{1}{2}$ | $\frac{1}{4}$ |
| C2 | 2g | $\frac{1}{2}$ | 0 | 0.144 |
| C3 | 2g | $\frac{1}{2}$ | 0 | 0.644 |

$$d(\text{Si-C}) = 1.83; d(\text{C-C}) = 1.65$$

c) Si_4C_4 (Figure 1c).

$$a = b = 3.090; c = 8.748$$

| Atomic site | Wyckoff | x | y | z |
|-------------|---------|---------------|---------------|---------------|
| C1 | 1a | 0 | 0 | 0 |
| C2 | 1d | 0 | 0 | $\frac{1}{2}$ |
| C3 | 2f | $\frac{1}{2}$ | $\frac{1}{2}$ | $\frac{1}{4}$ |
| Si1 | 2g | $\frac{1}{2}$ | 0 | 0.125 |
| Si2 | 2g | $\frac{1}{2}$ | 0 | 0.625 |

$$d(\text{Si-C}) = 1.89.$$

Table 1: Crystal parameters of tetragonal with space group $P-4m2$ N°115: C_8 , Si_8 , Si_2C_6 and Si_4C_4 from DFT calculations. Lattice constants and interatomic distances are given in units of Å ($1 \text{ \AA} = 10^{-10} \text{ m}$).

Computational framework

The investigations of the ground state unconstrained structures and the relevant physical properties were performed with plane-wave Vienna Ab initio Simulation Package (VASP) [9,10] based on the DFT. VASP uses the projector augmented wave (PAW) method for atomic potentials [10,11]. The DFT exchange-correlation (XC) effects were considered within generalized gradient approximation (GGA) [12]. The atoms were relaxed onto ground state geometry with a conjugate-gradient algorithm [13]. The Blöchl tetrahedron method [14] was applied for geometry optimization and energy calculations with corrections according to Methfessel-Paxton scheme [15]. A special kpoint sampling accounting for the geometry of the structures [16] was applied for approximating the reciprocal space Brillouin-zone (BZ) integrals. For better reliability, the optimization of the structural parameters was carried out along with successive self-consistent cycles with increasing mesh until the forces on atoms were less than 0.02 eV/\AA and the stress components lower than 0.003 eV/\AA^3 .

Besides the elastic constants calculated to infer the mechanical stabilities and hardness, further calculations of phonon dispersion curves were also carried out to verify the dynamic stability of the new carbon allotropes. In the present work, the phonon modes were computed considering the harmonic approximation via finite displacements of the atoms around their equilibrium positions to obtain the forces from the summation over the different configurations. The phonon dispersion curves along the direction of the Brillouin zone are subsequently obtained using "Phonopy" interface code [17] based on Python language. Lastly the electronic band structures were obtained with calculations with the all-electrons DFT-based augmented spherical method (ASW) [18].

Results and Discussions

Energy and crystal symmetry

As a first assessment, energy is a prevailing criterion.

The total energies in eV of C_8 , Si_4C_4 , Si_2C_6 , and Si_8 are -71.76, -60.27, -62.16 and -43.32, leading to atom-averaged cohesive energy E_{atom} (eV) of -2.495, -1.719, -1.565, and -0.385 respectively, after subtracting the atomic energies of C (-6.6 eV) and Si (-5.03 eV).

While all values are negative indicating cohesive chemical systems, noting that tetragonal C_8 is found energetically very close to diamond [19], the magnitudes drastically decrease in the series as Si replaces C, i.e., with the decrease of covalence, replaced by polar covalence in binary Si_2C_6 and Si_4C_4 ; nevertheless the latter (equiatomic) is found more cohesive than former.

The densities in g/cm^3 decrease concomitantly with Si amount: $\rho(C_8) = 3.53$, $\rho(Si_2C_6) = 3.32$, $\rho(Si_4C_4) = 3.193$, and $\rho(Si_8) = 2.285$. This is expected from the larger size of Si versus C as detailed above.

The resulting crystal structures are shown in figure 1a - 1d in ball-stick representation highlighting the tetrahedral 3D networks. Oppositely to the cubic structures of diamond, SiC and Si, the tetragonal novel structures are anisotropic with a large c/a ratio ~ 2.8 .

Table 1a details the crystal data of diamond and the new tetragonal C_8 and Si_8 showing 3 double and 2 single atomic positions. Such feature may become relevant upon undertaking selective substitutions modeling changes in diamond or intrinsic semi-conducting silicon in future works.

For an illustration, by removing C1 to simulate one carbon vacancy in diamond, the result after full geometry relaxation is the conservation of the C₇ structure while the cohesive energy E_{atom}(C₈) decreases strongly from -2.495 eV to E_{atom}(C₇) = -1.596 eV. Oppositely, by substituting Si to C1 to model SiC₇ there is a gain of cohesive energy; i.e., E_{atom}(SiC₇) = -1.896 eV is observed versus vacancy creation.

Developing on the binary silicon carbides, Si₂C₆ stoichiometry was obtained with the replacement of C1 and C2 (Table 1a, Wyckoff positions 1a and 1d) by Si1 Si2 (Table 1b) and Si₄C₄ stoichiometry was obtained by C occupying the two single Wyckoff positions 1a and 1d and one double Wyckoff position 2f while the four Si were made to occupy two 2g Wyckoff positions as shown in Table 1c. The full geometry relaxation led to the results shown in tables 1b and 1c, without change of the atomic positions and intermediate Si-C distance (Å) between C₈ and Si₈: d(C-C) = 1.54 < d(Si-C) = 1.89 < d(Si-Si) = 2.37. Note that Si₂C₆ presents intermediate distances as it contains C-C connections besides Si-C with the results: d(Si-C) = 1.83 Å and d(C-C) = 1.65 Å.

Besides being cohesive, the novel phases need further assessment mechanically and dynamically as developed here below.

Charge density 3D projections

The “electronic ↔ crystal structure” relationship is further illustrated with the charge density projections. Figure 2 shows the charge density volumes around the atoms with yellow volumes. Examining covalent C₈ (Figure 2a) the charge density shows perfect sp³ tetrahedral shape around carbon. Oppositely, in Si₂C₆ (Figure 2b) and Si₄C₄ (Figure 2c) the expected charge transfer Si→C (cf. Introduction) leads to localization of charge on carbon and a less defined tetrahedral C(sp³) like. In Si₈ (Figure 2d), the charges show the shape of segments localized in between Si-Si ensuring for the chemical bond, featuring a charge density distribution different from C₈.

Mechanical properties

The investigation of the mechanical properties is based on calculating the elastic properties determined by performing finite distortions in the lattice structure and deriving the elastic constants from the strain-stress relationship. From averaging

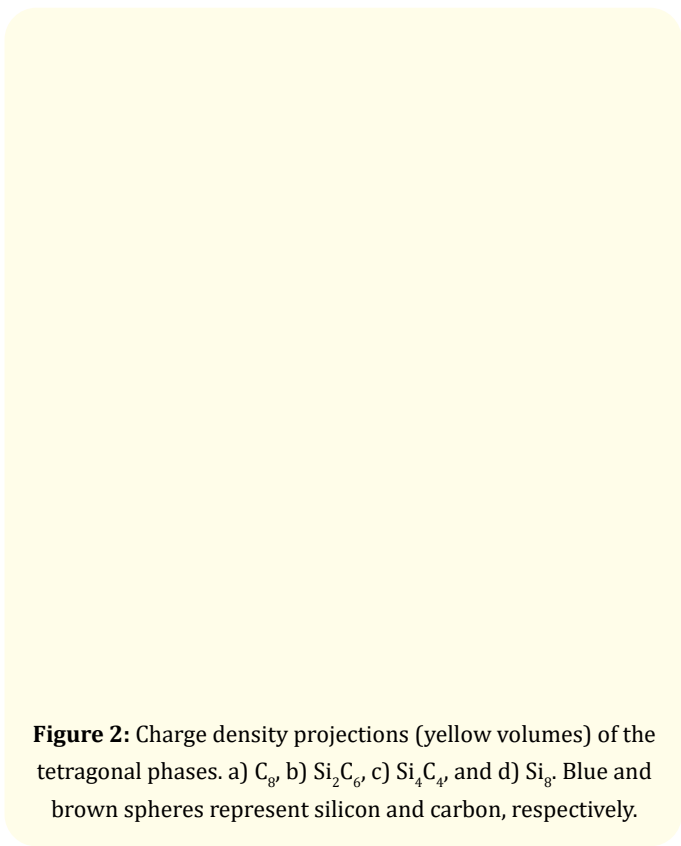


Figure 2: Charge density projections (yellow volumes) of the tetragonal phases. a) C₈, b) Si₂C₆, c) Si₄C₄, and d) Si₈. Blue and brown spheres represent silicon and carbon, respectively.

the elastic constants bulk (B) and shear (G) moduli are then obtained. For the averaging we used Voigt method [20] based on a uniform strain. The calculated sets of elastic constants are given in table 2. All values are positive. Their combinations obeying the rules pertaining to the mechanical stability of the phase, and the equations providing the bulk B_v and shear G_v moduli are as follows for the tetragonal system [21]:

| C _{ij} | C ₈ | Si ₂ C ₆ | Si ₄ C ₄ | Si ₈ |
|-----------------|----------------|--------------------------------|--------------------------------|-----------------|
| C ₁₁ | 1171 | 677 | 510 | 180 |
| C ₁₂ | 29 | 25 | 37 | 32 |
| C ₁₃ | 133 | 132 | 162 | 58 |
| C ₃₃ | 1067 | 675 | 422 | 153 |
| C ₄₄ | 465 | 176 | 127 | 48 |
| C ₆₆ | 567 | 343 | 246 | 73 |
| B _v | 444 | 290 | 241 | 90 |
| G _v | 582 | 303 | 208 | 65 |
| H _v | 113 | 51 | 34 | 13 |

Table 2: Elastic constants C_{ij} and Voigt values of bulk (B_v) and shear (G_v) moduli. The Vickers hardness (H_v) are provided in last column. All values are in GPa.

C_{ii} ($i=1, 3, 4, 6$) > 0 ; $C_{11} > C_{12}, C_{11} + C_{33} - 2C_{13} > 0$; and $2C_{11} + C_{33} + 2C_{12} + 4C_{13} > 0$.

$$B_{Voigt}^{tetr.} = 1/9 (2C_{11} + C_{33} + 2C_{12} + 4C_{13}),$$

$$\text{and } G_{Voigt}^{tetr.} = 1/15 (2C_{11} + C_{12} + 2C_{33} - 2C_{13} + 6C_{44} + 3C_{66}).$$

The calculated values are given in table 2. C₈ exhibits large $B_v = 444$ GPa and $G_v = 582$ GPa magnitudes. The calculated bulk modulus is equal to the value for diamond with $B_v = 445$ GPa but the calculated shear modulus is found much larger than G_v (diamond) = 550 GPa [22]. The consequence is that a larger hardness is expected for C₈. Regarding Si₄C₄ the values are close to SiC magnitudes in the literature [1]. Lastly Si₈ presents the lowest values of B_v and G_v close to the admitted values in the literature for cubic Si [23].

Based on these results, the Vickers hardness (H_v) was calculated with Chen-Niu [24] model using the B_v and G_v resulting from the elastic properties. The expression is:

$$H_v = 0.92 \cdot (G/B)^{1.137} \cdot G^{0.708}$$

The calculated H_v results are given in the last column of table 2. Clearly C₈ has the largest hardness magnitude due to the extremely large G_v , exceeding the diamond hardness which amounts to ~100 GPa [22]. It can be hypothesized that the anisotropic tetragonal structure characterized with a large tetragonality ratio of $c/a=2.8$ may be at the origin of the peculiar albeit interesting result, i.e., the growth of tetragonal C₈ with columnar elongated shape crystals would lead to extremely hard material; eventually for applications in cutting tools. Carbon rich Si₂C₆ on the other hand presents a high magnitude of hardness leading to consider it as a superhard material, better than Si₄C₄. Which possesses H_v magnitude close to c-SiC [1]. Lastly, the hardness magnitude of and Si₈ is close to literature values of cubic Si [23].

Dynamical stabilities from the phonons

Besides structural stability criteria observed for the new carbon allotrope from the positive magnitudes of the elastic constants and their combinations, the dynamical properties were also needed to provide complementary stability criteria. For the purpose, the phonons were subsequently computed. Phonons are quanta of vibrations; their energy is quantized through the Planck constant 'h' used in its reduced form \hbar ($\hbar = h/2\pi$) giving with the wave number ω the energy: $E = \hbar\omega$. Figure 3 shows the phonon band structures. Along the horizontal direction, the bands run along the major directions of the tetragonal Brillouin zone (reciprocal k-space). The

vertical direction shows the frequencies given in units of terahertz (THz). Since no negative frequency magnitudes are observed in the four panels, C₈ (Figure 3a), Si₂C₆ (Figure 3b), Si₄C₄ (Figure 3c), and Si₈ (Figure 3d) can be considered as dynamically stable. There are 3N-3 optical modes at higher energy than three acoustic modes starting from zero energy ($\omega = 0$) at the Γ point, center of the Brillouin Zone, up to a few Terahertz. They correspond to the lattice rigid translation modes of the crystal (two transverse and one longitudinal). The highest frequencies are observed for C₈ at 40 THz, a magnitude observed for diamond by Raman spectroscopy: $\omega \sim 40$ THz [25]. Upon decrease of carbon amount the highest frequency decreases, reaching the lowest values for Si₈ at ~15 THz, close to silicon intense Raman shift at 495 cm⁻¹.

Figure 3: Phonon band structures of along tetragonal Brillouin zone a) C_8 , b) Si_2C_6 , c) Si_4C_4 , and d) Si_8 .

Electronic band structures

Figure 4 shows the electronic band structures obtained with the calculated lattice constants using the ASW method [18]. The energy level along the vertical line is with respect to the top of the valence band (VB), E_v signaling a filled valence band with integer multiples of 8 (see discussion on the isoelectronicity in the Introduction), leaving an empty conduction band CB. In figure 4a showing the band structure of C_8 , the band gap is ~ 5 eV alike diamond and indirect between Γ_{VB} and Z_{CB} . A more than half smaller indirect gap is observed for Si_2C_6 (Figure 4b), decreasing further upon increase of Si content in Si_4C_4 equiatomic and lastly in Si_8 (Figure 4c, 4d).

Figure 4: Electronic band structures along the major lines of the tetragonal Brillouin zone. a) C_8 , b) Si_2C_6 , c) Si_4C_4 , and d) Si_8 .

Conclusions

In this work novel tetragonal allotropes and phases were proposed within the Si-C system, based on exhaustive investigations with DFT-based computations. From cohesive energies, mechanical and dynamic properties as well as electronic band structures, the four systems C_8 , Si_2C_6 , Si_4C_4 , and Si_8 were proven stable. While C_8 carbon allotrope is identified as ultra-hard alike diamond, Si_8 is found soft while the binaries Si_2C_6 and Si_4C_4 had intermediate Vickers hardness with a largest magnitude for Si_2C_6 allowing to

qualify it as superhard. It can be concluded that the C-Si system presents novel tetragonal allotropes of C and Si and two binary Si-C characterized with a broad range of mechanical properties likely to lead to applications. Lastly one could note that the softening induced by the increasing amount of Si herein can be approached to that observed in two-dimensional borophene (boron sheets) and similar systems that attracted great attention in recent years [26].

Bibliography

1. M Baloga, *et al.* "Nano- versus macro-hardness of liquid phase sintered SiC". *Journal of the European Ceramic Society* 25 (2005): 529-534.
2. Shuangshuang Zhang, *et al.* "CALYPSO software". *Chinese Physics B* 28 (2019): 106104.
3. AR Oganov. "Crystal structure prediction: reflections on present status and challenges". *Faraday Discuss* 211 (2018): 643.
4. P Hohenberg and W Kohn. "Inhomogeneous electron gas". *Physical Review B* 136 (1964) 864-871.
5. W Kohn and LJ Sham. "Self-consistent equations including exchange and correlation effects". *Physical Review A* 140 (1965): 1133-1138.
6. SF Matar and VL Solozhenko. "Crystal chemistry and first principles devising of C₄ as the simplest dense carbon allotrope". *Journal of Solid State Chemistry* 314 (2022): 123424.
7. T Yang, *et al.* "Gas phase formation of c-SiC₃ molecules in the circumstellar envelope of carbon stars". *PNAS (Proceedings of the National Academy of Sciences)* 116.29 (2019): 14471-14478.
8. SF Matar, *et al.* "First-principles investigations of tricarbon: From the isolated C₃ molecule to a novel ultra-hard anisotropic solid". *Carbon Trends* 6 (2022): 100132.
9. G Kresse, *et al.* "Efficient iterative schemes for ab initio total-energy calculations using a plane-wave basis set". *Physical Review B* 54 (1996): 11169.
10. G Kresse and J Joubert. "From ultrasoft pseudopotentials to the projector augmented wave". *Physical Review B* 59 (1999): 1758-1775.
11. PE Blöchl. "Projector augmented wave method". *Physical Review B* 50 (1994): 17953-17979.
12. J Perdew, *et al.* "The Generalized Gradient Approximation made simple". *Physical Review Letter* 77 (1996): 3865-3868.
13. WH Press, *et al.* "Numerical Recipes". 2nd ed. Cambridge University Press: New York, USA, (1986).
14. PE Blöchl, *et al.* "Improved tetrahedron method for Brillouin-zone integrations". *Physical Review B* 49 (1994): 16223-16233.
15. M Methfessel and AT Paxton. "High-precision sampling for Brillouin-zone integration in metals". *Physical Review B* 40 (1989): 3616-3621.
16. HJ Monkhorst and JD Pack. "Special k-points for Brillouin Zone integration". *Physical Review B* 13 (1976): 5188-5192.
17. A Togo and I Tanaka. "First principles phonon calculations in materials science". *Scripta Materialia* 108 (2015): 1-5.
18. V Eyert. "Basic notions and applications of the augmented spherical wave method". *International Journal of Quantum Chemistry* 77 (2000): 1007-1031.
19. SF Matar and VL Solozhenko. "Crystal chemistry rationale and ab initio investigation of ultra-hard dense rhombohedral carbon and boron nitride". *Diamond and Related Materials* 120 (2021): 108607.
20. W Voigt. "Über die Beziehung zwischen den beiden Elasticitätsconstanten isotroper Körper". *Annals Physics* 274 (1889): 573-587.
21. DC Wallace. "Thermodynamics of crystals". New York, USA: John Wiley and Sons (1972).
22. VV Brazhkin and VL Solozhenko. "Myths about new ultrahard phases: Why materials that are significantly superior to diamond in elastic moduli and hardness are impossible". *Journal of Applied Physics* 125 (2019): 130901.
23. Silicon - Strength - Hardness - Elasticity - Crystal Structure (material-properties.org).
24. X-Q Chen, *et al.* "Modeling hardness of polycrystalline materials and bulk metallic glasses". *Intermetallics* 19 (2011): 1275-1281.
25. RS Krishnan. "Raman spectrum of diamond". *Nature* 155 (1945): 171.
26. Dengfeng Li, *et al.* "Stretch-Driven Increase in Ultrahigh Thermal Conductance of Hydrogenated Borophene and Dimensionality Crossover in Phonon Transmission". *Advanced Functional Materials* 28.31 (2018): 1801685.